



University
of Glasgow

LHCb Collaboration.

Alexander, M., Borghi, S., Eklund, L., Pappagallo, M., Plackett, R., Rodrigues, E., Soler, F.J.P., and Spradlin, P. (2013) *Branching fraction and CP asymmetry of the decays $B^+ \rightarrow K^0_S \pi$ and $B^+ K \rightarrow 0_S K^+$* . Physics Letters B, 726 (4-5). pp. 646-655. ISSN 0370-2693

Copyright © 2013 CERN

<http://eprints.gla.ac.uk/87396/>

Deposited on: 20 November 2013



Branching fraction and CP asymmetry of the decays $B^+ \rightarrow K_S^0 \pi^+$ and $B^+ \rightarrow K_S^0 K^+$ [☆]



LHCb Collaboration

ARTICLE INFO

Article history:

Received 6 August 2013

Received in revised form 10 September 2013

Accepted 21 September 2013

Available online 30 September 2013

Editor: L. Rolandi

ABSTRACT

An analysis of $B^+ \rightarrow K_S^0 \pi^+$ and $B^+ \rightarrow K_S^0 K^+$ decays is performed with the LHCb experiment. The pp collision data used correspond to integrated luminosities of 1 fb^{-1} and 2 fb^{-1} collected at centre-of-mass energies of $\sqrt{s} = 7 \text{ TeV}$ and $\sqrt{s} = 8 \text{ TeV}$, respectively. The ratio of branching fractions and the direct CP asymmetries are measured to be $\mathcal{B}(B^+ \rightarrow K_S^0 K^+)/\mathcal{B}(B^+ \rightarrow K_S^0 \pi^+) = 0.064 \pm 0.009 \text{ (stat.)} \pm 0.004 \text{ (syst.)}$, $\mathcal{A}^{CP}(B^+ \rightarrow K_S^0 \pi^+) = -0.022 \pm 0.025 \text{ (stat.)} \pm 0.010 \text{ (syst.)}$ and $\mathcal{A}^{CP}(B^+ \rightarrow K_S^0 K^+) = -0.21 \pm 0.14 \text{ (stat.)} \pm 0.01 \text{ (syst.)}$. The data sample taken at $\sqrt{s} = 7 \text{ TeV}$ is used to search for $B_c^+ \rightarrow K_S^0 K^+$ decays and results in the upper limit $(f_c \cdot \mathcal{B}(B_c^+ \rightarrow K_S^0 K^+))/(f_u \cdot \mathcal{B}(B^+ \rightarrow K_S^0 \pi^+)) < 5.8 \times 10^{-2}$ at 90% confidence level, where f_c and f_u denote the hadronisation fractions of a \bar{b} quark into a B_c^+ or a B^+ meson, respectively.

© 2013 CERN. Published by Elsevier B.V. All rights reserved.

1. Introduction

Studies of charmless two-body B meson decays allow tests of the Cabibbo–Kobayashi–Maskawa picture of CP violation [1,2] in the Standard Model (SM). They include contributions from loop amplitudes, and are therefore particularly sensitive to processes beyond the SM [3–7]. However, due to the presence of poorly known hadronic parameters, predictions of CP violating asymmetries and branching fractions are imprecise. This limitation may be overcome by combining measurements from several charmless two-body B meson decays and using flavour symmetries [3]. More precise measurements of the branching fractions and CP violating asymmetries will improve the determination of the size of $SU(3)$ breaking effects and the magnitudes of colour-suppressed and annihilation amplitudes [8,9].

In $B^+ \rightarrow K_S^0 K^+$ and $B^+ \rightarrow K_S^0 \pi^+$ decays,¹ gluonic loop, colour-suppressed electroweak loop and annihilation amplitudes contribute. Measurements of their branching fractions and CP asymmetries allow to check for the presence of sizeable contributions from the latter two [6]. Further flavour symmetry checks can also be performed by studying these decays [10]. First measurements have been performed by the BaBar and Belle experiments [11,12]. The world averages are $\mathcal{A}^{CP}(B^+ \rightarrow K_S^0 \pi^+) = -0.015 \pm 0.019$, $\mathcal{A}^{CP}(B^+ \rightarrow K_S^0 K^+) = 0.04 \pm 0.14$ and $\mathcal{B}(B^+ \rightarrow K_S^0 K^+)/\mathcal{B}(B^+ \rightarrow K_S^0 \pi^+) = 0.050 \pm 0.008$, where

$$\mathcal{A}^{CP}(B^+ \rightarrow K_S^0 \pi^+) \equiv \frac{\Gamma(B^- \rightarrow K_S^0 \pi^-) - \Gamma(B^+ \rightarrow K_S^0 \pi^+)}{\Gamma(B^- \rightarrow K_S^0 \pi^-) + \Gamma(B^+ \rightarrow K_S^0 \pi^+)} \quad (1)$$

and $\mathcal{A}^{CP}(B^+ \rightarrow K_S^0 K^+)$ is defined in an analogous way.

Since the annihilation amplitudes are expected to be small in the SM and are often accompanied by other topologies, they are difficult to determine unambiguously. These can however be measured cleanly in $B_c^+ \rightarrow K_S^0 K^+$ decays, where other amplitudes do not contribute. Standard Model predictions for the branching fractions of pure annihilation B_c^+ decays range from 10^{-8} to 10^{-6} depending on the theoretical approach employed [13].

In this Letter, a measurement of the ratio of branching fractions of $B^+ \rightarrow K_S^0 K^+$ and $B^+ \rightarrow K_S^0 \pi^+$ decays with the LHCb detector is reported along with a determination of their CP asymmetries. The data sample corresponds to integrated luminosities of 1 and 2 fb^{-1} , recorded during 2011 and 2012 at centre-of-mass energies of 7 and 8 TeV, respectively. A search for the pure annihilation decay $B_c^+ \rightarrow K_S^0 K^+$ based on the data collected at 7 TeV is also presented. The $B^+ \rightarrow K_S^0 K^+$ and $B_c^+ \rightarrow K_S^0 K^+$ signal regions, along with the raw CP asymmetries, were not examined until the event selection and the fit procedure were finalised.

2. Detector, data sample and event selection

The LHCb detector [14] is a single-arm forward spectrometer covering the pseudorapidity range $2 < \eta < 5$, designed for the study of particles containing b or c quarks. The detector includes a high-precision tracking system consisting of a silicon-strip vertex detector (VELO) surrounding the pp interaction region, a large-area silicon-strip detector located upstream of a dipole magnet with a

[☆] © CERN for the benefit of the LHCb Collaboration.

¹ The inclusion of charge conjugated decay modes is implied throughout this Letter unless otherwise stated.

bending power of about 4 Tm, and three stations of silicon-strip detectors and straw drift tubes placed downstream. The magnetic field polarity is regularly flipped to reduce the effect of detection asymmetries. The pp collision data recorded with each of the two magnetic field polarities correspond to approximately half of the data sample. The combined tracking system provides a momentum measurement with relative uncertainty that varies from 0.4% at 5 GeV/c to 0.6% at 100 GeV/c, and an impact parameter resolution of 20 μm for tracks with high transverse momentum (p_T). Charged hadrons are identified using two ring-imaging Cherenkov detectors [15]. Photon, electron and hadron candidates are identified by a calorimeter system consisting of scintillating-pad and preshower detectors, an electromagnetic calorimeter and a hadronic calorimeter. Muons are identified by a system composed of alternating layers of iron and multiwire proportional chambers.

Simulated samples are used to determine efficiencies and the probability density functions (PDFs) used in the fits. The pp collisions are generated using PYTHIA 6.4 [16] with a specific LHCb-configuration [17]. Decays of hadronic particles are described by EVTGEN [18], in which final state radiation is generated using PHOTOS [19]. The interaction of the generated particles with the detector and its response are implemented using the GEANT4 toolkit [20] as described in Ref. [21].

The trigger [22] consists of a hardware stage, based on information from the calorimeter and muon systems, followed by a software stage, which performs a full event reconstruction. The candidates used in this analysis are triggered at the hardware stage either directly by one of the particles from the B candidate decay depositing a transverse energy of at least 3.6 GeV in the calorimeters, or by other activity in the event (usually associated with the decay products of the other b -hadron decay produced in the $pp \rightarrow b\bar{b}X$ interaction). Inclusion of the latter category increases the acceptance of signal decays by approximately a factor two. The software trigger requires a two- or three-particle secondary vertex with a high scalar sum of the p_T of the particles and significant displacement from the primary pp interaction vertices (PVs). A multivariate algorithm [23] is used for the identification of secondary vertices consistent with the decay of a b hadron.

Candidate $B^+ \rightarrow K_S^0 \pi^+$ and $B^+ \rightarrow K_S^0 K^+$ decays are formed by combining a $K_S^0 \rightarrow \pi^+ \pi^-$ candidate with a charged track that is identified as a pion or kaon, respectively. Only tracks in a fiducial volume with small detection asymmetries [24] are accepted in the analysis. Pions used to reconstruct the K_S^0 decays are required to have momentum $p > 2$ GeV/c, $\chi_{\text{IP}}^2 > 9$, and track segments in the VELO and in the downstream tracking chambers. The χ_{IP}^2 is defined as the difference in χ^2 of a given PV reconstructed with and without the considered particle. The K_S^0 candidates have $p > 8$ GeV/c, $p_T > 0.8$ GeV/c, a good quality vertex fit, a mass within ± 15 MeV/c² of the known value [25], and are well-separated from all PVs in the event. It is also required that their momentum vectors do not point back to any of the PVs in the event.

Pion and kaon candidate identification is based on the information provided by the RICH detectors [15], combined in the difference in the logarithms of the likelihoods for the kaon and pion hypotheses ($\text{DLL}_{K\pi}$). A track is identified as a pion (kaon) if $\text{DLL}_{K\pi} \leq 3$ ($\text{DLL}_{K\pi} > 3$), and $p < 110$ GeV/c, a momentum beyond which there is little separation between pions and kaons. The efficiencies of these requirements are 95% and 82% for signal pions and kaons, respectively. The misidentification probabilities of pions to kaons and kaons to pions are 5% and 18%. These figures are determined using a large sample of $D^{*+} \rightarrow D^0(\rightarrow K^- \pi^+) \pi^+$ decays reweighted by the kinematics of the simulated signal decays. Tracks that are consistent with particles leaving hits in the muon

detectors are rejected. Pions and kaons are also required to have $p_T > 1$ GeV/c and $\chi_{\text{IP}}^2 > 2$.

The B candidates are required to have the scalar p_T sum of the K_S^0 and the π^+ (or K^+) candidates that exceeds 4 GeV/c, to have $\chi_{\text{IP}}^2 < 10$ and $p > 25$ GeV/c and to form a good-quality vertex well separated from all the PVs in the event and displaced from the associated PV by at least 1 mm. The daughter (K_S^0 or π^+/K^+) with the larger p_T is required to have an impact parameter above 50 μm . The angle θ_{dir} between the B candidate's line of flight and its momentum is required to be less than 32 mrad. Background for K_S^0 candidates is further reduced by requiring the K_S^0 decay vertex to be significantly displaced from the reconstructed B decay vertex along the beam direction (z -axis), with $S_z \equiv (z_{K_S^0} - z_B) / \sqrt{\sigma_{z,K_S^0}^2 + \sigma_{z,B}^2} > 2$, where $\sigma_{z,K_S^0}^2$ and $\sigma_{z,B}^2$ are the uncertainties on the z positions of the K_S^0 and B decay vertices $z_{K_S^0}$ and z_B , respectively.

Boosted decision trees (BDT) [26] are trained using the AdaBoost algorithm [27] to further separate signal from background. The discriminating variables used are the following: S_z ; the χ_{IP}^2 of the K_S^0 and π^+/K^+ candidates; p_T , $\cos(\theta_{\text{dir}})$, χ_{VS}^2 of the B candidates defined as the difference in χ^2 of fits in which the B^+ decay vertex is constrained to coincide with the PV or not; and the imbalance of p_T , $A_{p_T} \equiv (p_T(B) - \sum p_T) / (p_T(B) + \sum p_T)$ where the scalar p_T sum is for all the tracks not used to form the B candidate and which lie in a cone around the B momentum vector. This cone is defined by a circle of radius 1 unit in the pseudorapidity-azimuthal angle plane, where the azimuthal angle is measured in radians. Combinatorial background tends to be less isolated with smaller p_T imbalance than typical b -hadron decays. The background training samples are taken from the upper B invariant mass sideband region in data ($5450 < m_B < 5800$ MeV/c²), while those of the signal are taken from simulated $B^+ \rightarrow K_S^0 \pi^+$ and $B^+ \rightarrow K_S^0 K^+$ decays. Two discriminants are constructed to avoid biasing the background level in the upper B mass sideband while making maximal use of the available data for training the BDT. The $K_S^0 \pi^+$ and $K_S^0 K^+$ samples are merged to prepare the two BDTs. They are trained using two independent equal-sized subsamples, each corresponding to half of the whole data sample. Both BDT outputs are found to be in agreement with each other in all aspects and each of them is applied to the other sample. For each event not used to train the BDTs, one of the two BDT outputs is arbitrarily applied. In this way, both BDT discriminants are applied to equal-sized data samples and the number of events used to train the BDTs is maximised without bias of the sideband region and the simulated samples used for the efficiency determination. The choice of the requirement on the BDT output (Q) is performed independently for the $K_S^0 \pi^\pm$ and $K_S^0 K^\pm$ samples by evaluating the signal significance $N_S / \sqrt{N_S + N_B}$, where N_S (N_B) denotes the expected number of signal (background) candidates. The predicted effective pollution from mis-identified $B^+ \rightarrow K_S^0 \pi^+$ decays in the $B^+ \rightarrow K_S^0 K^+$ signal mass region is taken into account in the calculation of N_B . The expected signal significance is maximised by applying $Q > 0.4$ (0.8) for $B^+ \rightarrow K_S^0 \pi^+$ ($B^+ \rightarrow K_S^0 K^+$) decays.

3. Asymmetries and signal yields

The CP -summed $B^+ \rightarrow K_S^0 K^+$ and $B^+ \rightarrow K_S^0 \pi^+$ yields are measured together with the raw charge asymmetries by means of a simultaneous unbinned extended maximum likelihood fit to the B^\pm candidate mass distributions of the four possible final states ($B^\pm \rightarrow K_S^0 \pi^\pm$ and $B^\pm \rightarrow K_S^0 K^\pm$). Five components contribute to each of the mass distributions. The signal is described by the sum

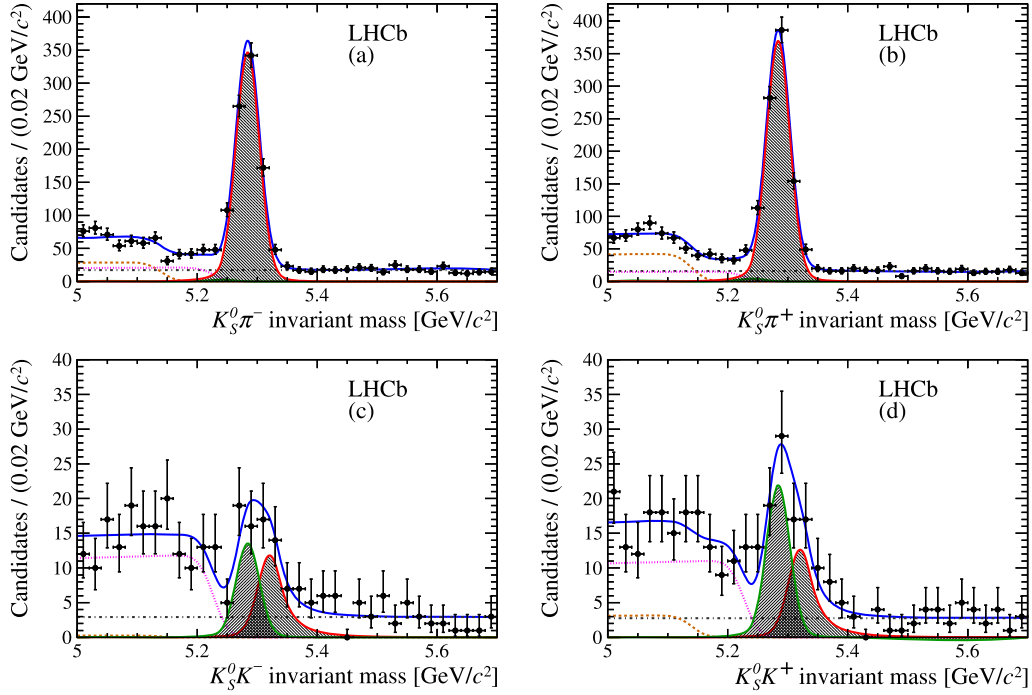


Fig. 1. Invariant mass distributions of selected (a) $B^- \rightarrow K_S^0 \pi^-$, (b) $B^+ \rightarrow K_S^0 \pi^+$, (c) $B^- \rightarrow K_S^0 K^-$ and (d) $B^+ \rightarrow K_S^0 K^+$ candidates. Data are points with error bars, the $B^+ \rightarrow K_S^0 \pi^+$ ($B^+ \rightarrow K_S^0 K^+$) components are shown as red falling hatched (green rising hatched) curves, combinatorial background is grey dash-dotted, partially reconstructed B_s^0 (B^0/B^+) backgrounds are dotted magenta (dashed orange). (For interpretation of the references to color in this figure legend, the reader is referred to the web version of this Letter.)

of a Gaussian distribution and a Crystal Ball function (CB) [28] with identical peak positions determined in the fit. The CB component models the radiative tail. The other parameters, which are determined from fits of simulated samples, are common for both decay modes. The width of the CB function is, according to the simulation, fixed to be 0.43 times that of the Gaussian distribution, which is left free in the fit.

Due to imperfect particle identification, $B^+ \rightarrow K_S^0 \pi^+$ ($B^+ \rightarrow K_S^0 K^+$) decays can be misidentified as $K_S^0 K^+$ ($K_S^0 \pi^+$) candidates. The corresponding PDFs are empirically modelled with the sum of two CB functions. For the $B^+ \rightarrow K_S^0 \pi^+$ ($B^+ \rightarrow K_S^0 K^+$) decay, the misidentification shape has a significant high (low) mass tail. The parameters of the two CB functions are determined from the simulation, and then fixed in fits to data.

Partially reconstructed decays, coming mainly from B^0 and B^+ (labelled B in this section), and B_s^0 meson decays to open charm and to a lesser extent from three-body charmless B and B_s^0 decays, are modelled with two PDFs. These PDFs are identical in the four possible final states. They are modelled by a step function with a threshold mass equal to $m_B - m_\pi$ ($m_{B_s^0} - m_\pi$) [25] for B (B_s^0) decays, convolved with a Gaussian distribution of width 20 MeV/ c^2 to account for detector resolution effects. Backgrounds from Λ_b^0 decays are found to be negligible. The combinatorial background is assumed to have a flat distribution in all categories.

The signal and background yields are varied in the fit, apart from those of the cross-feed contributions, which are constrained using known ratios of selection efficiencies from the simulation and particle identification and misidentification probabilities. The ratio of $B^+ \rightarrow K_S^0 K^+$ ($B^+ \rightarrow K_S^0 \pi^+$) events reconstructed and selected as $K_S^0 \pi^+$ ($K_S^0 K^+$) with respect to $K_S^0 K^+$ ($K_S^0 \pi^+$) are 0.245 ± 0.018 (0.0418 ± 0.0067), where the uncertainties are dominated by the finite size of the simulated samples. These numbers appear in Gaussian terms inserted in the fit likelihood function. The charge asymmetries of the backgrounds vary independently in the

fit, apart from those of the cross-feed contributions, which are identical to those of the properly reconstructed signal decay.

Fig. 1 shows the four invariant mass distributions along with the projections of the fit. The measured width of the Gaussian distribution used in the signal PDF is found to be approximately 20% larger than in the simulation, and is included as a systematic uncertainty. The CP -summed $B^+ \rightarrow K_S^0 \pi^+$ and $B^+ \rightarrow K_S^0 K^+$ signal yields are found to be $N(B^+ \rightarrow K_S^0 \pi^+) = 1804 \pm 47$ and $N(B^+ \rightarrow K_S^0 K^+) = 90 \pm 13$, with raw CP asymmetries $\mathcal{A}_{\text{raw}}(B^+ \rightarrow K_S^0 \pi^+) = -0.032 \pm 0.025$ and $\mathcal{A}_{\text{raw}}(B^+ \rightarrow K_S^0 K^+) = -0.23 \pm 0.14$. All background asymmetries are found to be consistent with zero within two standard deviations. By dividing the sample in terms of data taking periods and magnet polarity, no discrepancies of more than two statistical standard deviations are found in the raw CP asymmetries.

4. Corrections and systematic uncertainties

The ratio of branching fractions is determined as

$$\frac{\mathcal{B}(B^+ \rightarrow K_S^0 K^+)}{\mathcal{B}(B^+ \rightarrow K_S^0 \pi^+)} = \frac{N(B^+ \rightarrow K_S^0 K^+)}{N(B^+ \rightarrow K_S^0 \pi^+)} \cdot r_{\text{sel}} \cdot r_{\text{PID}}, \quad (2)$$

where the ratio of selection efficiencies is factorised into two terms representing the particle identification,

$$r_{\text{PID}} \equiv \frac{\varepsilon_{\text{PID}}(B^+ \rightarrow K_S^0 \pi^+)}{\varepsilon_{\text{PID}}(B^+ \rightarrow K_S^0 K^+)}, \quad (3)$$

and the rest of the selection,

$$r_{\text{sel}} \equiv \frac{\varepsilon_{\text{sel}}(B^+ \rightarrow K_S^0 \pi^+)}{\varepsilon_{\text{sel}}(B^+ \rightarrow K_S^0 K^+)}. \quad (4)$$

The raw CP asymmetries of the $B^+ \rightarrow K_S^0 \pi^+$ and $B^+ \rightarrow K_S^0 K^+$ decays are corrected for detection and production asymmetries

$\mathcal{A}_{\text{det+prod}}$, as well as for a small contribution due to CP violation in the neutral kaon system ($\mathcal{A}_{K_S^0}$). The latter is assumed to be the same for both $B^+ \rightarrow K_S^0 \pi^+$ and $B^+ \rightarrow K_S^0 K^+$ decays. At first order, the $B^+ \rightarrow K_S^0 \pi^+ CP$ asymmetry can be written as

$$\begin{aligned} \mathcal{A}^{CP}(B^+ \rightarrow K_S^0 \pi^+) &\approx \mathcal{A}_{\text{raw}}(B^+ \rightarrow K_S^0 \pi^+) \\ &\quad - \mathcal{A}_{\text{det+prod}}(B^+ \rightarrow K_S^0 \pi^+) \\ &\quad + \mathcal{A}_{K_S^0} \end{aligned}$$

and similarly for $B^+ \rightarrow K_S^0 K^+$, up to a sign flip in front of $\mathcal{A}_{K_S^0}$.

Selection efficiencies are determined from simulated samples generated at a centre-of-mass energy of 8 TeV. The ratio of selection efficiencies is found to be $r_{\text{sel}} = 1.111 \pm 0.019$, where the uncertainty is from the limited sample sizes. To first order, effects from imperfect simulation should cancel in the ratio of efficiencies. In order to assign a systematic uncertainty for a potential deviation of the ratio of efficiencies in 7 TeV data with respect to 8 TeV, the $B^+ \rightarrow K_S^0 \pi^+$ and $B^+ \rightarrow K_S^0 K^+$ simulated events are reweighted by a linear function of the B -meson momentum such that the average B momentum is 13% lower, corresponding to the ratio of beam energies. The 0.7% relative difference between the nominal and reweighted efficiency ratio is assigned as a systematic uncertainty. The distribution of the BDT output for simulated $B^+ \rightarrow K_S^0 \pi^+$ events is found to be consistent with the observed distribution of signal candidates in the data using the *sPlot* technique [29], where the discriminating variable is taken to be the B invariant mass. The total systematic uncertainty related to the selection is 1.8%.

The determination of the trigger efficiencies is subject to variations in the data-taking conditions and, in particular, to the ageing of the calorimeter system. These effects are mitigated by regular changes in the gain of the calorimeter system. A large sample of $D^{*+} \rightarrow D^0(\rightarrow K^- \pi^+) \pi^+$ decays is used to measure the trigger efficiency in bins of p_T for pions and kaons from signal decays. These trigger efficiencies are averaged using the p_T distributions obtained from simulation. The hardware stage trigger efficiencies obtained by this procedure are in agreement with those obtained in the simulation within 1.1%, which is assigned as systematic uncertainty on the ratio of branching fractions. The same procedure is also applied to B^+ and B^- decays separately, and results in 0.5% systematic uncertainty on the determination of the CP asymmetries.

Particle identification efficiencies are determined using a large sample of $D^{*+} \rightarrow D^0(\rightarrow K^- \pi^+) \pi^+$ decays. The kaons and pions from this calibration sample are reweighted in 18 bins of momentum and 4 bins of pseudorapidity, according to the distribution of signal kaons and pions from simulated $B^+ \rightarrow K_S^0 K^+$ and $B^+ \rightarrow K_S^0 \pi^+$ decays. The ratio of efficiencies is $r_{\text{PID}} = 1.154 \pm 0.025$, where the uncertainty is given by the limited size of the simulated samples. The systematic uncertainty associated with the binning scheme is determined by computing the deviation of the average efficiency calculated using the nominal binning from that obtained with a single bin in each kinematic variable. A variation of 0.7% (1.3%) is observed for pions (kaons). A systematic uncertainty of 0.5% is assigned due to variations of the efficiencies, determined by comparing results obtained with the 2011 and 2012 calibration samples. All these contributions are added in quadrature to obtain 2.7% relative systematic uncertainty on the particle identification efficiencies. Charge asymmetries due to the PID requirements are found to be negligible.

Uncertainties due to the modelling of the reconstructed invariant mass distributions are assigned by generating and fitting pseudo-experiments. Parameters of the signal and cross-feed dis-

tributions are varied according to results of independent fits to the $B^+ \rightarrow K_S^0 K^+$ and $B^+ \rightarrow K_S^0 \pi^+$ simulated samples. The relative uncertainty on the ratio of yields from mis-modelling of the signal (cross-feed) is 2.4% (2.7%) mostly affecting the small $B^+ \rightarrow K_S^0 K^+$ yield. The width of the Gaussian resolution function used to model the partially reconstructed backgrounds is increased by 20%, while the other fixed parameters of the partially reconstructed and combinatorial backgrounds are left free in the fit, in turn, to obtain a relative uncertainty of 3.3%. The total contribution of the fit model to the systematic uncertainty is 4.9%. Their contribution to the systematic uncertainties on the CP asymmetries is found to be negligible.

Detection and production asymmetries are measured using approximately one million $B^\pm \rightarrow J/\psi K^\pm$ decays collected in 2011 and 2012. Using a kinematic and topological selection similar to that employed in this analysis, a high purity sample is obtained. The raw CP asymmetry is measured to be $\mathcal{A}(B^\pm \rightarrow J/\psi K^\pm) = (-1.4 \pm 0.1)\%$ within 20 MeV/ c^2 of the B^+ meson mass. The same result is obtained by fitting the reconstructed invariant mass with a similar model to that used for the $B^+ \rightarrow K_S^0 \pi^+$ and $B^+ \rightarrow K_S^0 K^+$ fits. This asymmetry is consistent between bins of momentum and pseudorapidity within 0.5%, which is assigned as the corresponding uncertainty. The CP asymmetry in $B^\pm \rightarrow J/\psi K^\pm$ decays is $\mathcal{A}^{CP}(B^\pm \rightarrow J/\psi K^\pm) = (+0.5 \pm 0.3)\%$, where the value is the weighted average of the values from Refs. [25] and [30]. This leads to a correction of $\mathcal{A}_{\text{det+prod}}(B^+ \rightarrow K_S^0 K^+) = (-1.9 \pm 0.6)\%$. The combined production and detection asymmetry for $B^+ \rightarrow K_S^0 \pi^+$ decays is expressed as $\mathcal{A}_{\text{det+prod}}(B^+ \rightarrow K_S^0 \pi^+) = \mathcal{A}_{\text{det+prod}}(B^+ \rightarrow K_S^0 K^+) + \mathcal{A}_{K\pi}$, where the kaon-pion detection asymmetry is $\mathcal{A}_{K\pi} \approx \mathcal{A}_K - \mathcal{A}_\pi = (1.0 \pm 0.5)\%$ [31]. The assigned uncertainty takes into account a potential dependence of the difference of asymmetries as a function of the kinematics of the tracks. The total correction to $\mathcal{A}^{CP}(B^+ \rightarrow K_S^0 \pi^+)$ is $\mathcal{A}_{\text{det+prod}}(B^+ \rightarrow K_S^0 \pi^+) = (-0.9 \pm 0.8)\%$.

Potential effects from CP violation in the neutral kaon system, either directly via CP violation in the neutral kaon system [32] or via regeneration of a K_S^0 component through interactions of a K_L^0 state with material in the detector [33], are also considered. The former is estimated [34] by fitting the background subtracted [29] decay time distribution of the observed $B^+ \rightarrow K_S^0 \pi^+$ decays and contributes 0.1% to the observed asymmetry. The systematic uncertainty on this small effect is chosen to have the same magnitude as the correction itself. The latter has been studied [35] and is small for decays in the LHCb acceptance and thus no correction is applied. The systematic uncertainty assigned for this assumption is estimated by using the method outlined in Ref. [33]. Since the K_S^0 decays reconstructed in this analysis are concentrated at low lifetimes, the two effects are of similar sizes and have the same sign. Thus an additional systematic uncertainty equal to the size of the correction applied for CP violation in the neutral kaon system and 100% correlated with it, is assigned. It results in $\mathcal{A}_{K_S^0} = (0.1 \pm 0.2)\%$. A summary of the sources of systematic uncertainty and corrections to the CP asymmetries are given in Table 1. Total systematic uncertainties are calculated as the sum in quadrature of the individual contributions.

5. Search for $B_c^+ \rightarrow K_S^0 K^+$ decays

An exploratory search for $B_c^+ \rightarrow K_S^0 K^+$ decays is performed with the data sample collected in 2011, corresponding to an integrated luminosity of 1 fb $^{-1}$. The same selection as for the $B^+ \rightarrow K_S^0 K^+$ decays is used, only adding a proton veto $\text{DLL}_{pK} < 10$ to the K^+ daughter, which is more than 99% efficient. This is implemented to reduce a significant background from baryons in the

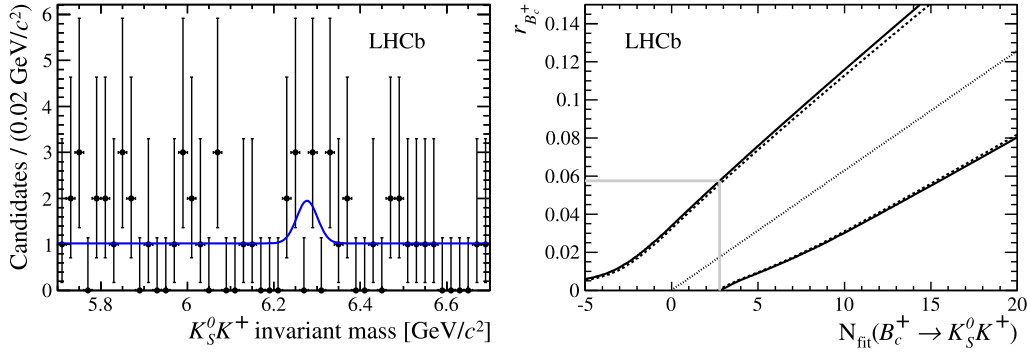


Fig. 2. (Left) Invariant mass distribution of selected $B_c^+ \rightarrow K_S^0 K^+$ candidates. Data are points with error bars and the curve represents the fitted function. (Right) The number of events and the corresponding value of $r_{B_c^+}$. The central value (dotted line) and the upper and lower 90% statistical confidence region bands are obtained using the Feldman and Cousins approach [36] (dashed lines). The solid lines includes systematic uncertainties. The gray outline of the box shows the obtained upper limit of $r_{B_c^+}$ for the observed number of 2.8 events.

Table 1

Corrections (above double line) and systematic uncertainties (below double line). The relative uncertainties on the ratio of branching fractions are given in the first column. The absolute corrections and related uncertainties on the CP asymmetries are given in the next two columns. The last column gathers the relative systematic uncertainties contributing to $r_{B_c^+}$. All values are given as percentages.

Source	\mathcal{B} ratio	$\mathcal{A}^{CP} B^+ \rightarrow K_S^0 \pi^+$	$\mathcal{A}^{CP} B^+ \rightarrow K_S^0 K^+$	B_c^+
$\mathcal{A}_{\text{det+prod}}$	–	–0.9	–1.9	–
$\mathcal{A}_{K_S^0}$	–	0.1	0.1	–
Selection	1.8	–	–	6.1
Trigger	1.1	0.5	0.5	1.1
Particle identification	2.7	–	–	3.6
Fit model	4.9	–	–	2.0
$\mathcal{A}_{\text{det+prod}}$	–	0.8	0.6	–
$\mathcal{A}_{K_S^0}$	–	0.2	0.2	–
Total syst. uncertainty	6.0	1.0	0.8	7.4

invariant mass region considered for this search. The ratios of selection and particle identification efficiencies are $r_{\text{sel}} = 0.306 \pm 0.012$ and $r_{\text{PID}} = 0.819 \pm 0.027$, where the uncertainties are from the limited size of the simulated samples. The related systematic uncertainties are estimated in a similar way as for the measurement of $\mathcal{B}(B^+ \rightarrow K_S^0 K^+)/\mathcal{B}(B^+ \rightarrow K_S^0 \pi^+)$. The $B^+ \rightarrow K_S^0 \pi^+$ yield is also evaluated with the 2011 data only. The B_c^+ signal yield is determined by fitting a single Gaussian distribution with the mean fixed to the B_c^+ mass [25] and the width fixed to 1.2 times the value obtained from simulation to take into account the worse resolution in data. The combinatorial background is assumed to be flat. The invariant mass distribution and the superimposed fit are presented in Fig. 2 (left). Pseudo-experiments are used to evaluate the biases in the fit procedure and the systematic uncertainties are evaluated by assuming that the combinatorial background has an exponential slope. A similar procedure is used to take into account an uncertainty related to the assumed width of the signal distribution. The 20% correction applied to match the observed resolution in data, is assumed to estimate this uncertainty.

The Feldman and Cousins approach [36] is used to build 90% confidence region bands that relate the true value of $r_{B_c^+} = (f_c \cdot \mathcal{B}(B_c^+ \rightarrow K_S^0 K^+))/(f_u \cdot \mathcal{B}(B^+ \rightarrow K_S^0 \pi^+))$ to the measured number of signal events, and where f_c and f_u are the hadronisation fraction of a b into a B_c^+ and a B^+ meson, respectively. All of the systematic uncertainties are included in the construction of the confidence region bands by inflating the width of the Gaussian functions used to build the ranking variable of the Feldman and Cousins procedure. The result is shown in Fig. 2 (right) and gives the upper limit

$$r_{B_c^+} \equiv \frac{f_c}{f_u} \cdot \frac{\mathcal{B}(B_c^+ \rightarrow K_S^0 K^+)}{\mathcal{B}(B^+ \rightarrow K_S^0 \pi^+)}$$

$$< 5.8 \times 10^{-2} \text{ at 90\% confidence level.}$$

This is the first upper limit on a B_c^+ meson decay into two light quarks.

6. Results and summary

The decays $B^+ \rightarrow K_S^0 K^+$ and $B^+ \rightarrow K_S^0 \pi^+$ have been studied using a data sample corresponding to an integrated luminosity of 3 fb^{-1} , collected in 2011 and 2012 by the LHCb detector and the ratio of branching fractions and CP asymmetries are found to be

$$\frac{\mathcal{B}(B^+ \rightarrow K_S^0 K^+)}{\mathcal{B}(B^+ \rightarrow K_S^0 \pi^+)} = 0.064 \pm 0.009 \text{ (stat.)} \pm 0.004 \text{ (syst.)},$$

$$\mathcal{A}^{CP}(B^+ \rightarrow K_S^0 \pi^+) = -0.022 \pm 0.025 \text{ (stat.)} \pm 0.010 \text{ (syst.)},$$

and

$$\mathcal{A}^{CP}(B^+ \rightarrow K_S^0 K^+) = -0.21 \pm 0.14 \text{ (stat.)} \pm 0.01 \text{ (syst.)}.$$

These results are compatible with previous determinations [11,12]. The measurements of $\mathcal{A}^{CP}(B^+ \rightarrow K_S^0 K^+)$ and $\mathcal{B}(B^+ \rightarrow K_S^0 K^+)/\mathcal{B}(B^+ \rightarrow K_S^0 \pi^+)$ are the best single determinations to date. A search for $B_c^+ \rightarrow K_S^0 K^+$ decays is also performed with a data sample corresponding to an integrated luminosity of 1 fb^{-1} . The upper limit

$$\frac{f_c}{f_u} \cdot \frac{\mathcal{B}(B_c^+ \rightarrow K_S^0 K^+)}{\mathcal{B}(B^+ \rightarrow K_S^0 \pi^+)} < 5.8 \times 10^{-2} \text{ at 90\% confidence level}$$

is obtained. Assuming $f_c \simeq 0.001$ [13], $f_u = 0.33$ [25,37,38], and $\mathcal{B}(B^+ \rightarrow K^0 \pi^+) = (23.97 \pm 0.53 \text{ (stat.)} \pm 0.71 \text{ (syst.)}) \times 10^{-6}$ [12], an upper limit $\mathcal{B}(B_c^+ \rightarrow \bar{K}^0 K^+) < 4.6 \times 10^{-4}$ at 90% confidence level is obtained. This is about two to four orders of magnitude higher than theoretical predictions, which range from 10^{-8} to 10^{-6} [13]. With the large data samples already collected by the LHCb experiment, other two-body B_c^+ decay modes to light quarks such as $B_c^+ \rightarrow \bar{K}^{*0} K^+$ and $B_c^+ \rightarrow \phi K^+$ may be searched for.

Acknowledgements

We express our gratitude to our colleagues in the CERN accelerator departments for the excellent performance of the LHC. We thank the technical and administrative staff at the LHCb institutes. We acknowledge support from CERN and from the national

agencies: CAPES, CNPq, FAPERJ and FINEP (Brazil); NSFC (China); CNRS/IN2P3 and Region Auvergne (France); BMBF, DFG, HGF and MPG (Germany); SFI (Ireland); INFN (Italy); FOM and NWO (The Netherlands); SCSR (Poland); MEN/IFA (Romania); MinES, Rosatom, RFBR and NRC “Kurchatov Institute” (Russia); MinECo, XuntaGal and GENCAT (Spain); SNSF and SER (Switzerland); NAS Ukraine (Ukraine); STFC (United Kingdom); NSF (USA). We also acknowledge the support received from the ERC under FP7. The Tier1 computing centres are supported by IN2P3 (France), KIT and BMBF (Germany), INFN (Italy), NWO and SURF (The Netherlands), PIC (Spain), GridPP (United Kingdom). We are thankful for the computing resources put at our disposal by Yandex LLC (Russia), as well as to the communities behind the multiple open source software packages that we depend on.

Open access

This article is published Open Access at [sciencedirect.com](https://www.sciencedirect.com). It is distributed under the terms of the Creative Commons Attribution License 3.0, which permits unrestricted use, distribution, and reproduction in any medium, provided the original authors and source are credited.

References

- [1] N. Cabibbo, Unitary symmetry and leptonic decays, *Phys. Rev. Lett.* **10** (1963) 531.
- [2] M. Kobayashi, T. Maskawa, CP-violation in the renormalizable theory of weak interaction, *Prog. Theor. Phys.* **49** (1973) 652.
- [3] R. Fleischer, New strategies to extract β and γ from $B_d \rightarrow \pi^+\pi^-$ and $B_s \rightarrow K^+K^-$, *Phys. Lett. B* **459** (1999) 306, arXiv:hep-ph/9903456.
- [4] M. Gronau, J.L. Rosner, The role of $B_s \rightarrow K\pi$ in determining the weak phase γ , *Phys. Lett. B* **482** (2000) 71, arXiv:hep-ph/0003119.
- [5] H.J. Lipkin, Is observed direct CP violation in $B_d \rightarrow K^+\pi^-$ due to new physics? Check Standard Model prediction of equal violation in $B_s \rightarrow K^-\pi^+$, *Phys. Lett. B* **621** (2005) 126, arXiv:hep-ph/0503022.
- [6] R. Fleischer, $B_{s,d} \rightarrow \pi\pi, \pi K, KK$: status and prospects, *Eur. Phys. J. C* **52** (2007) 267, arXiv:0705.1121.
- [7] R. Fleischer, R. Kneegjns, In pursuit of new physics with $B_s^0 \rightarrow K^+K^-$, *Eur. Phys. J. C* **71** (2011) 1532, arXiv:1011.1096.
- [8] A.J. Buras, R. Fleischer, S. Recksiegel, F. Schwab, $B \rightarrow \pi\pi$, new physics in $B \rightarrow \pi K$ and implications for rare K and B decays, *Phys. Rev. Lett.* **92** (2004) 101804, arXiv:hep-ph/0312259.
- [9] S. Baek, D. London, Is there still a $B \rightarrow \pi K$ puzzle?, *Phys. Lett. B* **653** (2007) 249, arXiv:hep-ph/0701181.
- [10] X.-G. He, S.-F. Li, H.-H. Lin, CP violation in $B_s^0 \rightarrow K^-\pi^+$, $B^0 \rightarrow K^+\pi^-$ decays and tests for SU(3) flavor symmetry predictions, arXiv:1306.2658.
- [11] BaBar Collaboration, B. Aubert, et al., Observation of $B^+ \rightarrow \bar{K}^0 K^+$ and $B^0 \rightarrow K^0 \bar{K}^0$, *Phys. Rev. Lett.* **97** (2006) 171805, arXiv:hep-ex/0608036.
- [12] Belle Collaboration, Y.-T. Duh, et al., Measurements of branching fractions and direct CP asymmetries for $B \rightarrow K\pi$, $B \rightarrow \pi\pi$ and $B \rightarrow KK$ decays, *Phys. Rev. D* **87** (2013) 031103, arXiv:1210.1348.
- [13] S. Descotes-Genon, J. He, E. Kou, P. Robbe, Nonleptonic charmless B_c decays and their search at LHCb, *Phys. Rev. D* **80** (2009) 114031, arXiv:0907.2256.
- [14] LHCb Collaboration, A.A. Alves Jr., et al., The LHCb detector at the LHC, *J. Instrum.* **3** (2008) S08005.
- [15] M. Adinolfi, et al., Performance of the LHCb RICH detector at the LHC, *Eur. Phys. J. C* **73** (2013) 2431, arXiv:1211.6759.
- [16] T. Sjöstrand, S. Mrenna, P. Skands, PYTHIA 6.4 physics and manual, *J. High Energy Phys.* **0605** (2006) 026, arXiv:hep-ph/0603175.
- [17] I. Belyaev, et al., Handling of the generation of primary events in Gauss, the LHCb simulation framework, in: Nuclear Science Symposium Conference Record (NSS/MIC), IEEE, 2010, p. 1155.
- [18] D.J. Lange, The EvtGen particle decay simulation package, *Nucl. Instrum. Methods A* **462** (2001) 152.
- [19] P. Golonka, Z. Was, PHOTOS Monte Carlo: a precision tool for QED corrections in Z and W decays, *Eur. Phys. J. C* **45** (2006) 97, arXiv:hep-ph/0506026.
- [20] Geant4 Collaboration, J. Allison, et al., Geant4 developments and applications, *IEEE Trans. Nucl. Sci.* **53** (2006) 270; Geant4 Collaboration, S. Agostinelli, et al., Geant4: a simulation toolkit, *Nucl. Instrum. Methods A* **506** (2003) 250.
- [21] M. Clemencic, et al., The LHCb simulation application, GAUSS: design, evolution and experience, *J. Phys. Conf. Ser.* **331** (2011) 032023.
- [22] R. Aaij, et al., The LHCb trigger and its performance in 2011, *J. Instrum.* **8** (2013) P04022, arXiv:1211.3055.
- [23] V.V. Gligorov, M. Williams, Efficient, reliable and fast high-level triggering using a bonsai boosted decision tree, *J. Instrum.* **8** (2013) P02013, arXiv:1210.6861.
- [24] LHCb Collaboration, R. Aaij, et al., Evidence for CP violation in time-integrated $D^0 \rightarrow h^- h^+$ decay rates, *Phys. Rev. Lett.* **108** (2012) 111602, arXiv:1112.0938.
- [25] Particle Data Group, J. Beringer, et al., Review of particle physics, *Phys. Rev. D* **86** (2012) 010001.
- [26] L. Breiman, J.H. Friedman, R.A. Olshen, C.J. Stone, Classification and regression trees, Wadsworth international group, Belmont, California, USA, 1984.
- [27] R.E. Schapire, Y. Freund, A decision-theoretic generalization of on-line learning and an application to boosting, *J. Comput. Syst. Sci.* **55** (1997) 119.
- [28] T. Skwarnicki, A study of the radiative cascade transitions between the Upsilon-prime and Upsilon resonances, PhD thesis, Institute of Nuclear Physics, Krakow, 1986, DESY-F31-86-02.
- [29] M. Pivk, F.R. Le Diberder, sPlot: a statistical tool to unfold data distributions, *Nucl. Instrum. Methods A* **555** (2005) 356, arXiv:physics/0402083.
- [30] DO Collaboration, V.M. Abazov, et al., Measurement of direct CP violation parameters in $B^\pm \rightarrow J/\psi K^\pm$ and $B^\pm \rightarrow J/\psi \pi^\pm$ decays with 10.4 fb⁻¹ of Tevatron data, *Phys. Rev. Lett.* **110** (2013) 241801, arXiv:1304.1655.
- [31] LHCb Collaboration, R. Aaij, et al., First observation of CP violation in the decays of B_s^0 strange mesons, *Phys. Rev. Lett.* **110** (2013) 221601, arXiv:1304.6173.
- [32] Y. Grossman, Y. Nir, CP violation in $\tau \rightarrow \nu \pi K_S^0$ and $D^- \rightarrow \pi K_S^0$: the importance of $K_S^0-K_L^0$ interference, *J. High Energy Phys.* **1204** (2012) 002, arXiv:1110.3790.
- [33] B. Ko, E. Won, B. Golob, P. Pakhlov, Effect of nuclear interactions of neutral kaons on CP asymmetry measurements, *Phys. Rev. D* **84** (2011) 111501, arXiv:1006.1938.
- [34] LHCb Collaboration, R. Aaij, et al., Measurement of the D^\pm production asymmetry in 7 TeV pp collisions, *Phys. Lett. B* **718** (2013) 902–909, arXiv:1210.4112.
- [35] LHCb Collaboration, R. Aaij, et al., Searches for CP violation in the $D^+ \rightarrow \phi\pi^+$ and $D_s^+ \rightarrow K_S^0\pi^+$ decays, *J. High Energy Phys.* **1306** (2013) 112, arXiv:1303.4906.
- [36] G.J. Feldman, R.D. Cousins, Unified approach to the classical statistical analysis of small signals, *Phys. Rev. D* **57** (1998) 3873, arXiv:physics/9711021.
- [37] LHCb Collaboration, R. Aaij, et al., Measurement of b hadron production fractions in 7 TeV pp collisions, *Phys. Rev. D* **85** (2012) 032008, arXiv:1111.2357.
- [38] LHCb Collaboration, R. Aaij, et al., Measurement of the fragmentation fraction ratio f_s/f_d and its dependence on B meson kinematics, *J. High Energy Phys.* **1304** (2013) 1, arXiv:1301.5286.

LHCb Collaboration

R. Aaij⁴⁰, B. Adeva³⁶, M. Adinolfi⁴⁵, C. Adrover⁶, A. Affolder⁵¹, Z. Ajaltouni⁵, J. Albrecht⁹, F. Alessio³⁷, M. Alexander⁵⁰, S. Ali⁴⁰, G. Alkhazov²⁹, P. Alvarez Cartelle³⁶, A.A. Alves Jr^{24,37}, S. Amato², S. Amerio²¹, Y. Amhis⁷, L. Anderlini^{17,f}, J. Anderson³⁹, R. Andreassen⁵⁶, J.E. Andrews⁵⁷, R.B. Appleby⁵³, O. Aquines Gutierrez¹⁰, F. Archilli¹⁸, A. Artamonov³⁴, M. Artuso⁵⁸, E. Aslanides⁶, G. Auriemma^{24,m}, M. Baalouch⁵, S. Bachmann¹¹, J.J. Back⁴⁷, C. Baesso⁵⁹, V. Balagura³⁰, W. Baldini¹⁶, R.J. Barlow⁵³, C. Barschel³⁷, S. Barsuk⁷, W. Barter⁴⁶, Th. Bauer⁴⁰, A. Bay³⁸, J. Beddow⁵⁰, F. Bedeschi²², I. Bediaga¹, S. Belogurov³⁰, K. Belous³⁴, I. Belyaev³⁰, E. Ben-Haim⁸, G. Bencivenni¹⁸, S. Benson⁴⁹, J. Benton⁴⁵, A. Berezhnoy³¹, R. Bernet³⁹, M.-O. Bettler⁴⁶, M. van Beuzekom⁴⁰, A. Bien¹¹, S. Bifani⁴⁴, T. Bird⁵³, A. Bizzeti^{17,h}, P.M. Bjørnstad⁵³,

T. Blake³⁷, F. Blanc³⁸, J. Blouw¹¹, S. Blusk⁵⁸, V. Bocci²⁴, A. Bondar³³, N. Bondar²⁹,
 W. Bonivento¹⁵, S. Borghi⁵³, A. Borgia⁵⁸, T.J.V. Bowcock⁵¹, E. Bowen³⁹, C. Bozzi¹⁶,
 T. Brambach⁹, J. van den Brand⁴¹, J. Bressieux³⁸, D. Brett⁵³, M. Britsch¹⁰, T. Britton⁵⁸,
 N.H. Brook⁴⁵, H. Brown⁵¹, I. Burducea²⁸, A. Bursche³⁹, G. Busetto^{21,q}, J. Buytaert³⁷,
 S. Cadeddu¹⁵, O. Callot⁷, M. Calvi^{20,j}, M. Calvo Gomez^{35,n}, A. Camboni³⁵,
 P. Campana^{18,37}, D. Campora Perez³⁷, A. Carbone^{14,c}, G. Carboni^{23,k}, R. Cardinale^{19,i},
 A. Cardini¹⁵, H. Carranza-Mejia⁴⁹, L. Carson⁵², K. Carvalho Akiba², G. Casse⁵¹,
 L. Castillo Garcia³⁷, M. Cattaneo³⁷, Ch. Cauet⁹, R. Cenci⁵⁷, M. Charles⁵⁴,
 Ph. Charpentier³⁷, P. Chen^{3,38}, N. Chiapolini³⁹, M. Chrzaszcz²⁵, K. Ciba³⁷, X. Cid Vidal³⁷,
 G. Ciezarek⁵², P.E.L. Clarke⁴⁹, M. Clemencic³⁷, H.V. Cliff⁴⁶, J. Closier³⁷, C. Coca²⁸,
 V. Coco⁴⁰, J. Cogan⁶, E. Cogneras⁵, P. Collins³⁷, A. Comerma-Montells³⁵, A. Contu^{15,37},
 A. Cook⁴⁵, M. Coombes⁴⁵, S. Coquereau⁸, G. Corti³⁷, B. Couturier³⁷, G.A. Cowan⁴⁹,
 D.C. Craik⁴⁷, S. Cunliffe⁵², R. Currie⁴⁹, C. D'Ambrosio³⁷, P. David⁸, P.N.Y. David⁴⁰,
 A. Davis⁵⁶, I. De Bonis⁴, K. De Bruyn⁴⁰, S. De Capua⁵³, M. De Cian¹¹, J.M. De Miranda¹,
 L. De Paula², W. De Silva⁵⁶, P. De Simone¹⁸, D. Decamp⁴, M. Deckenhoff⁹,
 L. Del Buono⁸, N. Déleage⁴, D. Derkach⁵⁴, O. Deschamps⁵, F. Dettori⁴¹, A. Di Canto¹¹,
 H. Dijkstra³⁷, M. Dogaru²⁸, S. Donleavy⁵¹, F. Dordei¹¹, A. Dosil Suárez³⁶, D. Dossett⁴⁷,
 A. Dovbnya⁴², F. Dupertuis³⁸, P. Durante³⁷, R. Dzhelyadin³⁴, A. Dziurda²⁵, A. Dzyuba²⁹,
 S. Easo⁴⁸, U. Egede⁵², V. Egorychev³⁰, S. Eidelman³³, D. van Eijk⁴⁰, S. Eisenhardt⁴⁹,
 U. Eitschberger⁹, R. Ekelhof⁹, L. Eklund^{50,37}, I. El Rifai⁵, Ch. Elsasser³⁹, A. Falabella^{14,e},
 C. Färber¹¹, G. Fardell⁴⁹, C. Farinelli⁴⁰, S. Farry⁵¹, D. Ferguson⁴⁹, V. Fernandez Albor³⁶,
 F. Ferreira Rodrigues¹, M. Ferro-Luzzi³⁷, S. Filippov³², M. Fiore¹⁶, C. Fitzpatrick³⁷,
 M. Fontana¹⁰, F. Fontanelli^{19,i}, R. Forty³⁷, O. Francisco², M. Frank³⁷, C. Frei³⁷,
 M. Frosini^{17,f}, S. Furcas²⁰, E. Furfaro^{23,k}, A. Gallas Torreira³⁶, D. Galli^{14,c},
 M. Gandelman², P. Gandini⁵⁸, Y. Gao³, J. Garofoli⁵⁸, P. Garosi⁵³, J. Garra Tico⁴⁶,
 L. Garrido³⁵, C. Gaspar³⁷, R. Gauld⁵⁴, E. Gersabeck¹¹, M. Gersabeck⁵³, T. Gershon^{47,37},
 Ph. Ghez⁴, V. Gibson⁴⁶, L. Giubega²⁸, V.V. Gligorov³⁷, C. Göbel⁵⁹, D. Golubkov³⁰,
 A. Golutvin^{52,30,37}, A. Gomes², P. Gorbounov^{30,37}, H. Gordon³⁷, C. Gotti²⁰,
 M. Grabalosa Gándara⁵, R. Graciani Diaz³⁵, L.A. Granado Cardoso³⁷, E. Graugés³⁵,
 G. Graziani¹⁷, A. Grecu²⁸, E. Greening⁵⁴, S. Gregson⁴⁶, P. Griffith⁴⁴, O. Grünberg⁶⁰,
 B. Gui⁵⁸, E. Gushchin³², Yu. Guz^{34,37}, T. Gys³⁷, C. Hadjivasiliou⁵⁸, G. Haefeli³⁸,
 C. Haen³⁷, S.C. Haines⁴⁶, S. Hall⁵², B. Hamilton⁵⁷, T. Hampson⁴⁵,
 S. Hansmann-Menzemer¹¹, N. Harnew⁵⁴, S.T. Harnew⁴⁵, J. Harrison⁵³, T. Hartmann⁶⁰,
 J. He³⁷, T. Head³⁷, V. Heijne⁴⁰, K. Hennessy⁵¹, P. Henrard⁵, J.A. Hernando Morata³⁶,
 E. van Herwijnen³⁷, M. Hess⁶⁰, A. Hicheur¹, E. Hicks⁵¹, D. Hill⁵⁴, M. Hoballah⁵,
 C. Hombach⁵³, P. Hopchev⁴, W. Hulsbergen⁴⁰, P. Hunt⁵⁴, T. Huse⁵¹, N. Hussain⁵⁴,
 D. Hutchcroft⁵¹, D. Hynds⁵⁰, V. Iakovenko⁴³, M. Idzik²⁶, P. Ilten¹², R. Jacobsson³⁷,
 A. Jaeger¹¹, E. Jans⁴⁰, P. Jaton³⁸, A. Jawahery⁵⁷, F. Jing³, M. John⁵⁴, D. Johnson⁵⁴,
 C.R. Jones⁴⁶, C. Joram³⁷, B. Jost³⁷, M. Kaballo⁹, S. Kandybei⁴², W. Kanso⁶, M. Karacson³⁷,
 T.M. Karbach³⁷, I.R. Kenyon⁴⁴, T. Ketel⁴¹, A. Keune³⁸, B. Khanji²⁰, O. Kochebina⁷,
 I. Komarov³⁸, R.F. Koopman⁴¹, P. Koppenburg⁴⁰, M. Korolev³¹, A. Kozlinskiy⁴⁰,
 L. Kravchuk³², K. Kreplin¹¹, M. Kreps⁴⁷, G. Krocker¹¹, P. Krokovny³³, F. Kruse⁹,
 M. Kucharczyk^{20,25,j}, V. Kudryavtsev³³, T. Kvaratskheliya^{30,37}, V.N. La Thi³⁸,
 D. Lacarrere³⁷, G. Lafferty⁵³, A. Lai¹⁵, D. Lambert⁴⁹, R.W. Lambert⁴¹, E. Lanciotti³⁷,
 G. Lanfranchi¹⁸, C. Langenbruch³⁷, T. Latham⁴⁷, C. Lazzeroni⁴⁴, R. Le Gac⁶,
 J. van Leerdam⁴⁰, J.-P. Lees⁴, R. Lefèvre⁵, A. Leflat³¹, J. Lefrançois⁷, S. Leo²², O. Leroy⁶,
 T. Lesiak²⁵, B. Leverington¹¹, Y. Li³, L. Li Gioi⁵, M. Liles⁵¹, R. Lindner³⁷, C. Linn¹¹,
 B. Liu³, G. Liu³⁷, S. Lohn³⁷, I. Longstaff⁵⁰, J.H. Lopes², N. Lopez-March³⁸, H. Lu³,
 D. Lucchesi^{21,q}, J. Luisier³⁸, H. Luo⁴⁹, F. Machefert⁷, I.V. Machikhiliyan^{4,30}, F. Maciuc²⁸,
 O. Maev^{29,37}, S. Malde⁵⁴, G. Manca^{15,d}, G. Mancinelli⁶, J. Maratas⁵, U. Marconi¹⁴,
 P. Marino^{22,s}, R. Märki³⁸, J. Marks¹¹, G. Martellotti²⁴, A. Martens^{8,*}, A. Martín Sánchez⁷,
 M. Martinelli⁴⁰, D. Martinez Santos⁴¹, D. Martins Tostes², A. Martynov³¹,

A. Massafferri¹, R. Matev³⁷, Z. Mathe³⁷, C. Matteuzzi²⁰, E. Maurice⁶,
 A. Mazurov^{16,32,37,e}, J. McCarthy⁴⁴, A. McNab⁵³, R. McNulty¹², B. McSkelly⁵¹,
 B. Meadows^{56,54}, F. Meier⁹, M. Meissner¹¹, M. Merk⁴⁰, D.A. Milanese⁸, M.-N. Minard⁴,
 J. Molina Rodriguez⁵⁹, S. Monteil⁵, D. Moran⁵³, P. Morawski²⁵, A. Mordà⁶,
 M.J. Morello^{22,s}, R. Mountain⁵⁸, I. Mous⁴⁰, F. Muheim⁴⁹, K. Müller³⁹, R. Muresan²⁸,
 B. Muryn²⁶, B. Muster³⁸, P. Naik⁴⁵, T. Nakada³⁸, R. Nandakumar⁴⁸, I. Nasteva¹,
 M. Needham⁴⁹, S. Neubert³⁷, N. Neufeld³⁷, A.D. Nguyen³⁸, T.D. Nguyen³⁸,
 C. Nguyen-Mau^{38,o}, M. Nicol⁷, V. Niess⁵, R. Niet⁹, N. Nikitin³¹, T. Nikodem¹¹,
 A. Nomerotski⁵⁴, A. Novoselov³⁴, A. Oblakowska-Mucha²⁶, V. Obraztsov³⁴, S. Oggero⁴⁰,
 S. Ogilvy⁵⁰, O. Okhrimenko⁴³, R. Oldeman^{15,d}, M. Orlandea²⁸, J.M. Otalora Goicochea²,
 P. Owen⁵², A. Oyanguren³⁵, B.K. Pal⁵⁸, A. Palano^{13,b}, T. Palczewski²⁷, M. Palutan¹⁸,
 J. Panman³⁷, A. Papanestis⁴⁸, M. Pappagallo⁵⁰, C. Parkes⁵³, C.J. Parkinson⁵²,
 G. Passaleva¹⁷, G.D. Patel⁵¹, M. Patel⁵², G.N. Patrick⁴⁸, C. Patrignani^{19,i},
 C. Pavel-Nicorescu²⁸, A. Pazos Alvarez³⁶, A. Pellegrino⁴⁰, G. Penso^{24,l}, M. Pepe Altarelli³⁷,
 S. Perazzini^{14,c}, E. Perez Trigo³⁶, A. Pérez-Calero Yzquierdo³⁵, P. Perret⁵,
 M. Perrin-Terrin⁶, L. Pescatore⁴⁴, E. Pesen⁶¹, K. Petridis⁵², A. Petrolini^{19,i}, A. Phan⁵⁸,
 E. Picatoste Olloqui³⁵, B. Pietrzyk⁴, T. Pilař⁴⁷, D. Pinci²⁴, S. Playfer⁴⁹, M. Plo Casasus³⁶,
 F. Polci⁸, G. Polok²⁵, A. Poluektov^{47,33}, E. Polycarpo², A. Popov³⁴, D. Popov¹⁰,
 B. Popovici²⁸, C. Potterat³⁵, A. Powell⁵⁴, J. Prisciandaro³⁸, A. Pritchard⁵¹, C. Prouve⁷,
 V. Pugatch⁴³, A. Puig Navarro³⁸, G. Punzi^{22,r}, W. Qian⁴, J.H. Rademacker⁴⁵,
 B. Rakotomiaramanana³⁸, M.S. Rangel², I. Raniuk⁴², N. Rauschmayr³⁷, G. Raven⁴¹,
 S. Redford⁵⁴, M.M. Reid⁴⁷, A.C. dos Reis¹, S. Ricciardi⁴⁸, A. Richards⁵², K. Rinnert⁵¹,
 V. Rives Molina³⁵, D.A. Roa Romero⁵, P. Robbe⁷, D.A. Roberts⁵⁷, E. Rodrigues⁵³,
 P. Rodriguez Perez³⁶, S. Roiser³⁷, V. Romanovsky³⁴, A. Romero Vidal³⁶, J. Rouvinet³⁸,
 T. Ruf³⁷, F. Ruffini²², H. Ruiz³⁵, P. Ruiz Valls³⁵, G. Sabatino^{24,k}, J.J. Saborido Silva³⁶,
 N. Sagidova²⁹, P. Sail⁵⁰, B. Saitta^{15,d}, V. Salustino Guimaraes², B. Sanmartin Sedes³⁶,
 M. Sannino^{19,i}, R. Santacesaria²⁴, C. Santamarina Rios³⁶, E. Santovetti^{23,k}, M. Sapunov⁶,
 A. Sarti^{18,l}, C. Satriano^{24,m}, A. Satta²³, M. Savrie^{16,e}, D. Savrina^{30,31}, P. Schaack⁵²,
 M. Schiller⁴¹, H. Schindler³⁷, M. Schlupp⁹, M. Schmelling¹⁰, B. Schmidt³⁷,
 O. Schneider³⁸, A. Schopper³⁷, M.-H. Schune⁷, R. Schwemmer³⁷, B. Sciascia¹⁸,
 A. Sciubba²⁴, M. Seco³⁶, A. Semennikov³⁰, K. Senderowska²⁶, I. Sepp⁵², N. Serra³⁹,
 J. Serrano⁶, P. Seyfert¹¹, M. Shapkin³⁴, I. Shapoval^{16,42}, P. Shatalov³⁰, Y. Shcheglov²⁹,
 T. Shears^{51,37}, L. Shekhtman³³, O. Shevchenko⁴², V. Shevchenko³⁰, A. Shires⁹,
 R. Silva Coutinho⁴⁷, M. Sirendi⁴⁶, N. Skidmore⁴⁵, T. Skwarnicki⁵⁸, N.A. Smith⁵¹,
 E. Smith^{54,48}, J. Smith⁴⁶, M. Smith⁵³, M.D. Sokoloff⁵⁶, F.J.P. Soler⁵⁰, F. Soomro¹⁸,
 D. Souza⁴⁵, B. Souza De Paula², B. Spaan⁹, A. Sparkes⁴⁹, P. Spradlin⁵⁰, F. Stagni³⁷,
 S. Stahl¹¹, O. Steinkamp³⁹, S. Stevenson⁵⁴, S. Stoica²⁸, S. Stone⁵⁸, B. Storaci³⁹,
 M. Straticiuc²⁸, U. Straumann³⁹, V.K. Subbiah³⁷, L. Sun⁵⁶, S. Swientek⁹, V. Syropoulos⁴¹,
 M. Szczekowski²⁷, P. Szczypka^{38,37}, T. Szumlak²⁶, S. T'Jampens⁴, M. Teklishyn⁷,
 E. Teodorescu²⁸, F. Teubert³⁷, C. Thomas⁵⁴, E. Thomas³⁷, J. van Tilburg¹¹, V. Tisserand⁴,
 M. Tobin³⁸, S. Tolk⁴¹, D. Tonelli³⁷, S. Topp-Joergensen⁵⁴, N. Torr⁵⁴, E. Tournefier^{4,52},
 S. Tourneur³⁸, M.T. Tran³⁸, M. Tresch³⁹, A. Tsaregorodtsev⁶, P. Tsopelas⁴⁰, N. Tuning⁴⁰,
 M. Ubeda Garcia³⁷, A. Ukleja²⁷, D. Urner⁵³, A. Ustyuzhanin^{52,p}, U. Uwer¹¹, V. Vagnoni¹⁴,
 G. Valenti¹⁴, A. Vallier⁷, M. Van Dijk⁴⁵, R. Vazquez Gomez¹⁸, P. Vazquez Regueiro³⁶,
 C. Vázquez Sierra³⁶, S. Vecchi¹⁶, J.J. Velthuis⁴⁵, M. Veltri^{17,g}, G. Veneziano³⁸,
 M. Vesterinen³⁷, B. Viaud⁷, D. Vieira², X. Vilasis-Cardona^{35,n}, A. Vollhardt³⁹,
 D. Volyanskyy¹⁰, D. Voong⁴⁵, A. Vorobyev²⁹, V. Vorobyev³³, C. Voß⁶⁰, H. Voss¹⁰,
 R. Waldi⁶⁰, C. Wallace⁴⁷, R. Wallace¹², S. Wandernoth¹¹, J. Wang⁵⁸, D.R. Ward⁴⁶,
 N.K. Watson⁴⁴, A.D. Webber⁵³, D. Websdale⁵², M. Whitehead⁴⁷, J. Wicht³⁷,
 J. Wiechczynski²⁵, D. Wiedner¹¹, L. Wiggers⁴⁰, G. Wilkinson⁵⁴, M.P. Williams^{47,48},
 M. Williams⁵⁵, F.F. Wilson⁴⁸, J. Wimberley⁵⁷, J. Wishahi⁹, W. Wislicki²⁷, M. Witek²⁵,
 S.A. Wotton⁴⁶, S. Wright⁴⁶, S. Wu³, K. Wyllie³⁷, Y. Xie^{49,37}, Z. Xing⁵⁸, Z. Yang³,

R. Young⁴⁹, X. Yuan³, O. Yushchenko³⁴, M. Zangoli¹⁴, M. Zavertyaev^{10,a}, F. Zhang³,
 L. Zhang⁵⁸, W.C. Zhang¹², Y. Zhang³, A. Zhelezov¹¹, A. Zhokhov³⁰, L. Zhong³,
 A. Zvyagin³⁷

¹ Centro Brasileiro de Pesquisas Físicas (CBPF), Rio de Janeiro, Brazil

² Universidade Federal do Rio de Janeiro (UFRJ), Rio de Janeiro, Brazil

³ Center for High Energy Physics, Tsinghua University, Beijing, China

⁴ LAPP, Université de Savoie, CNRS/IN2P3, Annecy-Le-Vieux, France

⁵ Clermont Université, Université Blaise Pascal, CNRS/IN2P3, LPC, Clermont-Ferrand, France

⁶ CPPM, Aix-Marseille Université, CNRS/IN2P3, Marseille, France

⁷ LAL, Université Paris-Sud, CNRS/IN2P3, Orsay, France

⁸ LPNHE, Université Pierre et Marie Curie, Université Paris Diderot, CNRS/IN2P3, Paris, France

⁹ Fakultät Physik, Technische Universität Dortmund, Dortmund, Germany

¹⁰ Max-Planck-Institut für Kernphysik (MPIK), Heidelberg, Germany

¹¹ Physikalisches Institut, Ruprecht-Karls-Universität Heidelberg, Heidelberg, Germany

¹² School of Physics, University College Dublin, Dublin, Ireland

¹³ Sezione INFN di Bari, Bari, Italy

¹⁴ Sezione INFN di Bologna, Bologna, Italy

¹⁵ Sezione INFN di Cagliari, Cagliari, Italy

¹⁶ Sezione INFN di Ferrara, Ferrara, Italy

¹⁷ Sezione INFN di Firenze, Firenze, Italy

¹⁸ Laboratori Nazionali dell'INFN di Frascati, Frascati, Italy

¹⁹ Sezione INFN di Genova, Genova, Italy

²⁰ Sezione INFN di Milano Bicocca, Milano, Italy

²¹ Sezione INFN di Padova, Padova, Italy

²² Sezione INFN di Pisa, Pisa, Italy

²³ Sezione INFN di Roma Tor Vergata, Roma, Italy

²⁴ Sezione INFN di Roma La Sapienza, Roma, Italy

²⁵ Henryk Niewodniczanski Institute of Nuclear Physics Polish Academy of Sciences, Kraków, Poland

²⁶ AGH – University of Science and Technology, Faculty of Physics and Applied Computer Science, Kraków, Poland

²⁷ National Center for Nuclear Research (NCBJ), Warsaw, Poland

²⁸ Horia Hulubei National Institute of Physics and Nuclear Engineering, Bucharest-Magurele, Romania

²⁹ Petersburg Nuclear Physics Institute (PNPI), Gatchina, Russia

³⁰ Institute of Theoretical and Experimental Physics (ITEP), Moscow, Russia

³¹ Institute of Nuclear Physics, Moscow State University (SINP MSU), Moscow, Russia

³² Institute for Nuclear Research of the Russian Academy of Sciences (INR RAN), Moscow, Russia

³³ Budker Institute of Nuclear Physics (SB RAS) and Novosibirsk State University, Novosibirsk, Russia

³⁴ Institute for High Energy Physics (IHEP), Protvino, Russia

³⁵ Universitat de Barcelona, Barcelona, Spain

³⁶ Universidad de Santiago de Compostela, Santiago de Compostela, Spain

³⁷ European Organization for Nuclear Research (CERN), Geneva, Switzerland

³⁸ Ecole Polytechnique Fédérale de Lausanne (EPFL), Lausanne, Switzerland

³⁹ Physik-Institut, Universität Zürich, Zürich, Switzerland

⁴⁰ Nikhef National Institute for Subatomic Physics, Amsterdam, The Netherlands

⁴¹ Nikhef National Institute for Subatomic Physics and VU University Amsterdam, Amsterdam, The Netherlands

⁴² NSC Kharkiv Institute of Physics and Technology (NSC KIPT), Kharkiv, Ukraine

⁴³ Institute for Nuclear Research of the National Academy of Sciences (KINR), Kyiv, Ukraine

⁴⁴ University of Birmingham, Birmingham, United Kingdom

⁴⁵ H.H. Wills Physics Laboratory, University of Bristol, Bristol, United Kingdom

⁴⁶ Cavendish Laboratory, University of Cambridge, Cambridge, United Kingdom

⁴⁷ Department of Physics, University of Warwick, Coventry, United Kingdom

⁴⁸ STFC Rutherford Appleton Laboratory, Didcot, United Kingdom

⁴⁹ School of Physics and Astronomy, University of Edinburgh, Edinburgh, United Kingdom

⁵⁰ School of Physics and Astronomy, University of Glasgow, Glasgow, United Kingdom

⁵¹ Oliver Lodge Laboratory, University of Liverpool, Liverpool, United Kingdom

⁵² Imperial College London, London, United Kingdom

⁵³ School of Physics and Astronomy, University of Manchester, Manchester, United Kingdom

⁵⁴ Department of Physics, University of Oxford, Oxford, United Kingdom

⁵⁵ Massachusetts Institute of Technology, Cambridge, MA, United States

⁵⁶ University of Cincinnati, Cincinnati, OH, United States

⁵⁷ University of Maryland, College Park, MD, United States

⁵⁸ Syracuse University, Syracuse, NY, United States

⁵⁹ Pontifícia Universidade Católica do Rio de Janeiro (PUC-Rio), Rio de Janeiro, Brazil [†]

⁶⁰ Institut für Physik, Universität Rostock, Rostock, Germany [‡]

⁶¹ Celal Bayar University, Manisa, Turkey [‡]

* Corresponding author.

E-mail address: aurelien.martens@lpnhe.in2p3.fr (A. Martens).

^a P.N. Lebedev Physical Institute, Russian Academy of Science (LPI RAS), Moscow, Russia.

^b Università di Bari, Bari, Italy.

^c Università di Bologna, Bologna, Italy.

^d Università di Cagliari, Cagliari, Italy.

^e Università di Ferrara, Ferrara, Italy.

^f Università di Firenze, Firenze, Italy.

^g Università di Urbino, Urbino, Italy.

^h Università di Modena e Reggio Emilia, Modena, Italy.

- ⁱ Università di Genova, Genova, Italy.
- ^j Università di Milano Bicocca, Milano, Italy.
- ^k Università di Roma Tor Vergata, Roma, Italy.
- ^l Università di Roma La Sapienza, Roma, Italy.
- ^m Università della Basilicata, Potenza, Italy.
- ⁿ LIFAELS, La Salle, Universitat Ramon Llull, Barcelona, Spain.
- ^o Hanoi University of Science, Hanoi, Viet Nam.
- ^p Institute of Physics and Technology, Moscow, Russia.
- ^q Università di Padova, Padova, Italy.
- ^r Università di Pisa, Pisa, Italy.
- ^s Scuola Normale Superiore, Pisa, Italy.
- ^t Associated to Universidade Federal do Rio de Janeiro (UFRJ), Rio de Janeiro, Brazil.
- ^u Associated to Physikalisches Institut, Ruprecht-Karls-Universität Heidelberg, Heidelberg, Germany.
- ^v Associated to European Organization for Nuclear Research (CERN), Geneva, Switzerland.